UCRL-JRNL-208222

LAWRENCE
LIVERMORE
NATIONAL
LABORATORY

The effects of fill tubes on the hydrodynamics of ignition targets and prospects for ignition

M. J. Edwards, M. M. Marinak, T. Dittrich, S. Haan, J. Sanchez, J. Klingman, J. Moody

November 29, 2004

Physics of Plasmas

Disclaimer

This document was prepared as an account of work sponsored by an agency of the United States Government. Neither the United States Government nor the University of California nor any of their employees, makes any warranty, express or implied, or assumes any legal liability or responsibility for the accuracy, completeness, or usefulness of any information, apparatus, product, or process disclosed, or represents that its use would not infringe privately owned rights. Reference herein to any specific commercial product, process, or service by trade name, trademark, manufacturer, or otherwise, does not necessarily constitute or imply its endorsement, recommendation, or favoring by the United States Government or the University of California. The views and opinions of authors expressed herein do not necessarily state or reflect those of the United States Government or the University of California, and shall not be used for advertising or product endorsement purposes.

The effects of fill tubes on the hydrodynamics of ignition targets and prospects for ignition

John Edwards, Marty Marinak, Tom Dittrich, Steve Haan, Jorge Sanchez, Jeff Klingman, and John Moody

Lawrence Livermore National Laboratory, Livermore CA 94550, USA

Abstract

The notion of using a narrow bore fill tube to charge an ignition capsule in-situ with DT fuel is very attractive because it eliminates the need for cryogenic transport of the target from the filling station to the target chamber, and in principle is one way of allowing any material to be considered as an ablator. We are using the radiation hydrocode HYDRA in 2D to study the effect of fill-tubes on graded copper doped Be ignition capsule implosions. The capsule is ~ 1.1 mm radius, and driven at ~ 300 eV. Fill-tubes are made of glass and range in diameter from 10-20 μm. These are inserted between 5-40 μm into the ablator surface and a glue layer around the capsule ~ 2μm thick is included. The calculations are unusually demanding in that the flow is highly nonlinear from the outset, and very high angular resolution is necessary to capture the initial evolution of the tube, which is complex. Despite this complexity, the net result is that by the time the capsule implosion takes off, a preferred, simple Bessel-like mode is set up that is almost independent of, and much larger than, the initial tube size, and close to the fastest growing mode for the capsule. The perturbation continues to grow during the unstable acceleration phase, and inverts as the capsule begins to stagnate, sending a spike of cold DT into the forming hot-spot. In all cases studied the capsule ignites and gives close to clean 1D yield, and the perturbation growth is found to vary linearly with the diameter of the tube. The simulations and results are discussed.

For submission to the special issue of Physics of Plasmas for the DPP meeting of the APS in Savannah, GA, November 15-19th, 2004

This work was performed under the auspices of the U.S. Department of Energy by the University of California, Lawrence Livermore National Laboratory under contract No. W-7405-Eng-48.

I Introduction

The original concept for fielding cryogenic capsules on the National Ignition Facility (NIF) was to charge the target in a separate facility and then transport it at cryogenic temperatures to the target chamber to be shot [1]. This is doable and currently remains the longer-term plan, but will take some time to put in place. Over the last year or so we have begun investigating alternative options for cryogenic filling that will enable us to make ignition attempts shortly after the laser is completed. One of these is referred to as the fill tube option. In this scenario a small hole is drilled through the ablator and a fine glass tube, which is attached to the outside of the target, is used to deliver the fuel into the capsule at liquid DT temperatures right next to the target chamber (see Fig 1). As challenging as this sounds, progress over the last year suggests this is very much a realistic cryogenic option. A prototype cryo filling system has been designed, built and successfully fielded; a plastic 2 mm OD capsule was filled with liquid DT inside a hohlraum using a glass fill tube with a 25μm OD and 8 μm ID [2]. While simulations predict that there are target designs that would ignite with a tube very close to this size, other sources of "imperfection" in a real ignition attempt motivates even smaller tubes by ~ a factor of 2. Importantly we have been able to attach glass tubes of this size (~ 10 μm OD) to surrogate surfaces using a glue layer that is only ~ 1μm thick, with an insertion depth into the surface ~ 10μm [3]. In addition it has been possible to make the holes in the ablator necessary to flow the DT through using laser drilling. The smallest of these have been ~ 2μm diameter.

The main subject of this paper, however, is the result of design simulations of targets containing fill tubes and how the details of the tubes affect target performance. We consider tube diameter, depth of insertion into the ablator, and show some preliminary results for a conceptual Be tube. The results presented are for a graded copper-doped Be target, but we have performed limited studies on Be capsules with a spatially uniform copper dopant and a graded doped CH design, both of which behave similarly but are not quite as resistant to the fill-tube perturbation as the graded doped design. We have considered tubes up to 20 μm diameter, and all targets have ignited, and given close to 1D yield, although performance is degrading slightly as the tube size is increased. We find that the scaling of perturbation growth with tube diameter is linear, rather than the cubic scaling that might be expected from simple "added mass" arguments. The paper is arranged as follows. The capsule and computational set-up is described in section 2. We then present a case study of a HYDRA simulation of an implosion with a fill tube in section 3. The effect of tube size and insertion depth into the ablator is considered in section 4 and the results discussed in section 5 prior to concluding.

II Computational model

Most of the results presented in this paper will be for a graded copper-doped, 5-layer, Be capsule (Fig. 2). The x-ray drive peaks at 300 eV and the capsule absorbs ~ 180 kJ. This is similar to designs presented elsewhere [4], but the gas density is 0.5 mg/cc (rather than 0.3 mg/cc) corresponding to operation near the DT triple point. The clean 1D

yield is ~ 16 MJ, which is less than the ~ 20MJ obtained from a very similar capsule which has a gas density of 0.3 mg/cc. The hohlarum gas was taken to be He at a density of 1 mg/cc.

Several configurations (see table 1) were considered in this study with fill tubes made primarily of glass (SiO_2). The diameter of the tube was varied from ~10 μm up to ~20 μm keeping the depth of insertion fixed at 20 μm. For one tube size (B, 13.5 μm tube) the depth of insertion was also varied from 5μm up to 40 μm. A glue layer ~ 2μm thick was included around the tube in nearly all cases. The hole in the tube was given the same diameter as the hole running through the ablator, and they were made to be coaxial. In one case the hole in the ablator was removed as a numerical exercise to determine the effect of a jet that is formed when the hole is present.

	Tube OD (μm)	Tube ID (μm)	Glue layer (μm)	Insertion depth (μm)
A	10.1	3.4	1.7	20
B	13.5	5.0	1.7	20
C	16.9	6.7	2.5	20
D	20.2	8.4	3.4	20
E	13.5	5.0	1.7	5
F	13.5	5.0	1.7	40
G*	13.5	5.0	0.0	20

Table 1 Fill tube configurations considered in the design study presented here.
* case G tube is Be and there is no glue layer.

All components of the tube assembly were mesh aligned at t=0 so that the dimensions varied slightly with radial position. The mesh alignment was continued for ~ 100 μm above the surface of the capsule at which point the tube was mapped out to the hohlraum wall, which in this case was simulated by a rigid, spherical wall at the radius of the hohlraum (~ 3mm). Actual tubes that have been made by stretching micro-glass tubes (~ 100μm initial OD) exhibit a very slight taper. This increases the tube OD by much less than a factor of 2 over the ~ 2mm to the hohlraum wall. Omitting this slight taper in the simulations is not expected to change the results presented here, although much larger tapers might well do. This question will need to be answered in future studies.

The simulations were conducted in RZ geometry with the fill tube on axis. In order to calculate the capsule yield, a 180 degree segment was simulated. The baseline simulation included 432 radial, and 4096 computational cells equally spaced in angle (0.044 degrees). This was kept the same as the tube size was varied so that the effective resolution increased as the tube size increased. Simulations were also completed with twice the spatial resolution in the ablator, and gave the same answers as the lower resolution mesh. The radiation transport was treated in the diffusion approximation using 15 energy groups. Simulations using 30 groups gave almost identical answers, slightly

decreasing perturbation growth if anything. One simulation was also performed using an implicit monte carlo solver for the radiation field using 4 M photons. This was to determine the effect of long range shadowing of the capsule by the tube material that is not captured by the diffusion approximation. In this case only a 45 degree wedge was used. The drive spectrum was taken from a separate, integrated hohlraum simulation. Opacities were calculated using a screened hydrogenic model and the QEOS equation of state model was used.

Integrated 2D hohlraum simulations were also conducted to assess the effect of the fill-tube plasma on the capsule symmetry. In this case the fill tube plasma was simulated as a low density region of SiO_2 around the equator. The change in the implosion due to the inclusion of the fill tube plasma was slight, causing the core at ignition to be slightly "sausage" (Fig 3). These 2D calculations presumably over estimate the effect of a tube plasma because slightly more mass was included in the simulation than there would be from a tube. Further studies will be needed to confirm the preliminary conclusion that this is likely to be a relatively small effect.

III Case study of an implosion containing a fill-tube

In the following section we describe the sequence of events in a simulation that includes a fill-tube (case C, 17μm tube) (see Fig. 4). As the drive turns on, both the capsule and ablator begin to ablate, and the tube starts to implode. The portion of the target directly under the fill-tube is shielded from the drive and consequently does not ablate yet. The expansion of the Be is slightly faster than that of glass and the boundary between the glass and Be ablator makes an angle slightly less than 45 degrees to the tube axis as a result. The expansion of the tube plasma causes the shielded area to exceed that directly under the tube. This shielding continues until the tube in the hohlraum has expanded sufficiently to become transparent. At this time any long-range shadow cast by the tube material disappears, and the radiation shortly after begins to eat into the portion of the tube that is inside the ablator. The ablation of the glass is a little less efficient than that in the Be and the ablation front continues to lag behind that in the remainder of the ablator well away from the tube. Finally, all the remaining glass is ablated and there are no further sources to seed the perturbation. This occurs at ~ 12-13 ns in the case of the 17 μm tube, although the precise timing of this sequence depends of course on the size of the tube, and its composition.

As the shocks are launched into the ablator they run over the glass tube and then crush the hole in the ablator. Because the hole is filled with a lower density material, a jet is formed that propagates out ahead of the main shock front in the Be. This in turn causes a transverse shock to propagate out away from the hole. The jet passes into the DT ice and eventually out into the gas. This coincidentally happens at about the same time as the last of the glass tube in the ablator is burned away, which is also around the time the third shock is launched into the target. A small amount of Be, roughly equivalent to ~ 5μg/cc of material at t=0 is carried into the gas. At this level of contamination ignition will not be affected. However, the transport of ablator material into the gas is difficult to

calculate and should be the subject of further simulation, and ideally experimental validation.

As the fourth shock is launched the shell begins to accelerate inward collecting the jet material as it goes. By the peak of the drive ~ 15ns (Fig 4f), a preferred mode has developed, which as expected, is much larger than the original size of the tube. This continues to grow into a characteristic bubble and spike configuration as the implosion continues. This growth causes DT to flow up into the spike. Eventually the capsule enters the stagnation phase and the inward falling spike begins to penetrate what will become the hot spot. The spike is entirely DT, and as the temperature in the hot spot increases the spike begins to get eroded. It reaches a maximum penetration just before ignition when the ion temperature in the hot spot is ~ 9 keV. By the time ignition occurs (T_i~12 keV) the spike has been eroded almost right back to the inner surface of the low adiabat DT shell. The capsule then burns and this particular target gave 15.8 MJ yield, which is close to the 1D clean yield. All the cases studied behave in a qualitatively similar fashion.

IV Scaling of results with tube size and insertion depth

The size of the tube is much smaller than the most unstable capsule modes and it would be reasonable to expect the detailed shape of the tube to be unimportant in determining later perturbation growth. One notion is that the mass of the tube involved in seeding the perturbation acts to set the initial amplitude of the preferred scales that end up growing. If we assume that some length of tube proportional to the initial diameter is involved in setting the perturbed mass, then we would expect perturbation growth that was cubic in tube diameter for the 4 different tubes in cases A-D. If we had kept the tube wall thickness constant, the same argument would lead to a scaling that is quadratic in tube diameter. What we observe however is a scaling that is very close to linear in tube diameter. This is shown in Fig. 5a. Here we plot $(\rho R - \rho R_o)/\rho R_o = \delta\rho R/\rho R_o$ where ρR_o is the value in the unperturbed part of the implosion, at a time of 15 ns, which is close to peak drive. By this time the perturbation has settled into a preferred mode, much larger than the initial scale of the fill-tube. We also find that $\delta\rho R$ around this time is an excellent indicator of how the perturbation will appear near ignition. The dashed lines are scaled linearly from case B, and overlay the other curves almost exactly, suggesting a different seed mechanism. We also show the spike amplitude normalized to the unperturbed hot-spot radius defined by the 50% peak Ti contour in Fig 5b as a function of time near ignition. This also appears to exhibit a scaling that is nearly linear in tube size. The fact that the spike is being strongly eroded by thermal conduction in the hot spot makes this less compelling. Nevertheless, the scaling is certainly less than cubic.

The fact that the depth of insertion of the tube was kept fixed in cases A-D is not a contributing factor to the linear scaling we observe. The tube insertion was varied from 5μm up to 40 μm, and no significant differences were observed in the perturbation growth. This suggests that the principal mechanism for seeding the perturbation is the behavior of the tube outside the ablator.

V Discussion

In order to help elucidate the dominant mechanism for the perturbation seed mechanism further, we have conducted several additional simulations. In order to determine the effect of the jet that propagates down the fill hole in the ablator, a simulation identical to case B was carried out except the hole through the ablator was omitted. This simulation exhibited no jet but resulted in behavior almost indistinguishable from case B. This indicates that the hole and jet are not especially important. Because of this it is tempting to suggest that the mass perturbation seeded by the tube might be partially countered by increasing the size of the hole. While this is worthy of further investigation, it seems likely that the jet will begin to become important at some point as it gets larger, particularly as more ablator material would presumably be carried into the DT gas which would start to eat away ignition margin.

We have also considered an additional source of perturbation not properly captured by the diffusion treatment, long range shadowing of the ablator by the tube. In Fig 6 we show the fractional flux deficit vs polar angle away from the surface of the tube due to shadowing. This plot assumes that the tube is entirely opaque, which is a reasonable approximation at early time. Next to the tube only half the sky can be seen and the flux is reduced there by a factor of 2. As we travel away from the surface the deficit falls rapidly but is still surprisingly large at relatively large distances. We have verified using IMC calculations in hydra that the details of this shadowing are not reproduced at early time when the diffusion approximation is used. However, because the tube essentially blows up on a relatively short time scale this omission is totally swamped by the much larger effect of the local mass perturbation created by the tube shielding the ablator directly beneath it. In fact, when we compare $\delta\rho R$ vs polar angle after all sources of perturbation seed have finished (after ~ 12 ns), we find that IMC and diffusion simulations give very similar answers. We compare $\delta\rho R$ vs angle in Fig 7 for IMC and diffusion simulations at 13ns. The OD of the tube in these simulations was 10 μm. The wall thickness in the IMC calculation was slightly thinner than that in the diffusion calculation, but this is not a large effect. As can be seen it is hard to distinguish between the two calculations. We thus conclude that long range shadowing, at least for this size tube is not important. It is possible that the relative importance of long range shadowing increases as the tube size increases because it takes longer for the tube to explode and become transparent. This will need to be addressed in future simulations.

Finally, two additional simulations have been conducted that have the same dimension as case B. However, in one case the section of the tube inside the ablator and up to ~30μm outside the ablator was replaced with Be (the remainder of the tube was kept as glass). In the second simulation the entire tube was made of Be. No "glue" joints were included in either simulation. The first calculation gave almost identical answers to case B while the pure Be tube resulted in a very much reduced perturbation (Fig 8). Taken together with the other evidence presented this strongly suggests that the dominant seed mechanism is shielding of the ablator directly under the relatively opaque expanding tube plasma. This shielding lasts for as long as it takes for the tube to blow down and become transparent.

Clearly, additional simulations and analyses are necessary to understand in detail the observed linear scaling of the perturbation size with tube diameter. However, this behavior could be explained if the spatial scale of the shielding were independent of the initial tube size, and the time taken for the part of the tube outside the ablator responsible for shielding to become transparent were linearly dependent on the tube diameter.

VI Conclusions

We have presented 2D HYDRA simulations of ignition targets, which include glass fill-tubes with diameters ranging from 10 μm up to 20 μm. All of these targets have ignited and given yields close to the clean 1D yield. Together with recent cryogenic filling and target fabrication developments, these results make the fill tube option for fielding cryogenic capsules appear very promising.

The details of the early complex hydrodynamics of the tube assembly are apparently not important and a preferred mode ends up growing, which is much larger than, and unrelated to, the initial tube diameter. The amplitude of the perturbation is found to vary linearly with the diameter of the tube, rather than in a cubic fashion, which would be more consistent with a simple "added mass" argument. Instead, the simulations indicate that the dominant perturbation seed is the shielding that occurs directly under the expanding fill tube plasma until this plasma has expanded enough to become transparent. Further simulations and analyses are necessary to understand this fully.

This work was performed under the auspices of the U.S. Department of Energy by the University of California, Lawrence Livermore National Laboratory under contract No. W-7405-Eng-48.

References

1. J. D. Lindl, Phys. Plasmas **2**, 3933 (1995).
2. J. Sanchez et al., Bull Am Phys Soc EM2.006, 46th Meeting DPP, Savannah, GA 2004.
3. J. L. Klingman, J Reynolds, J Burmann, Bull Am Phys NP1.116, Soc, 46th Meeting DPP, Savannah, GA 2004.
4. S. W. Haan et al, Physics of Plasmas, this issue.

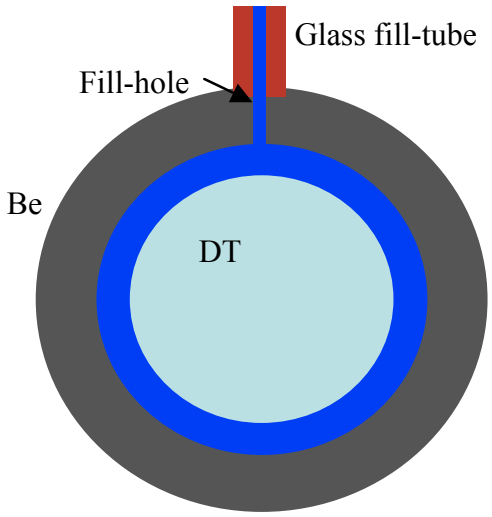

Fig 1 Schematic of fill tube concept

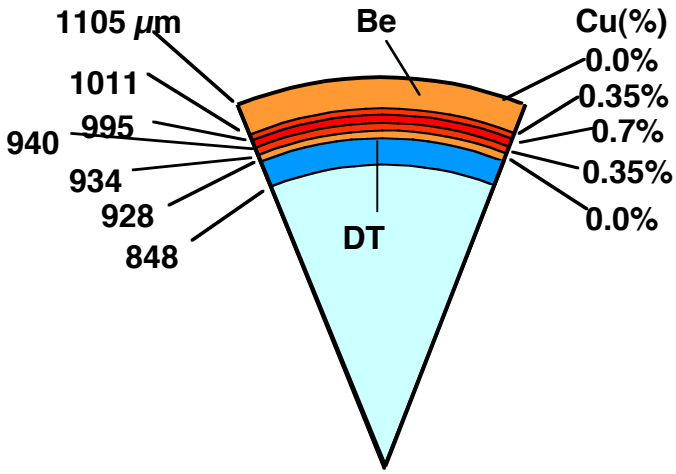

Fig 2a Schematic of graded copper doped Be capsule

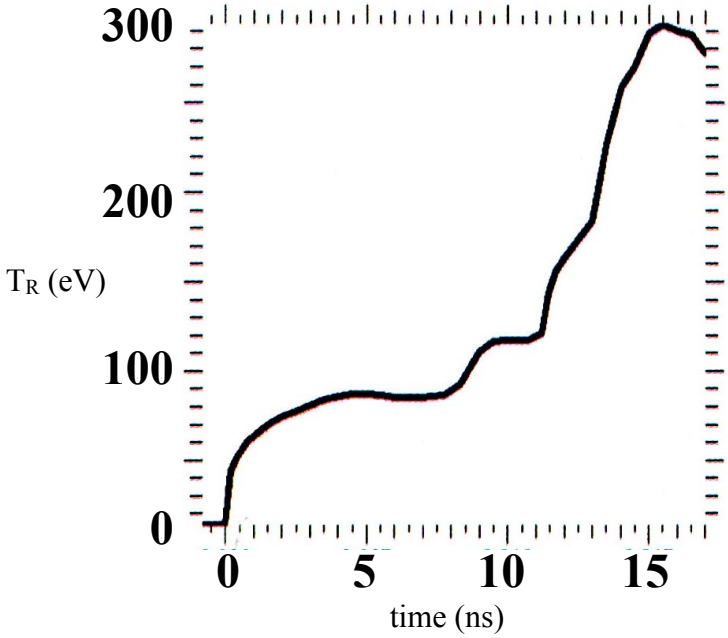

Fig 2b. Capsule drive

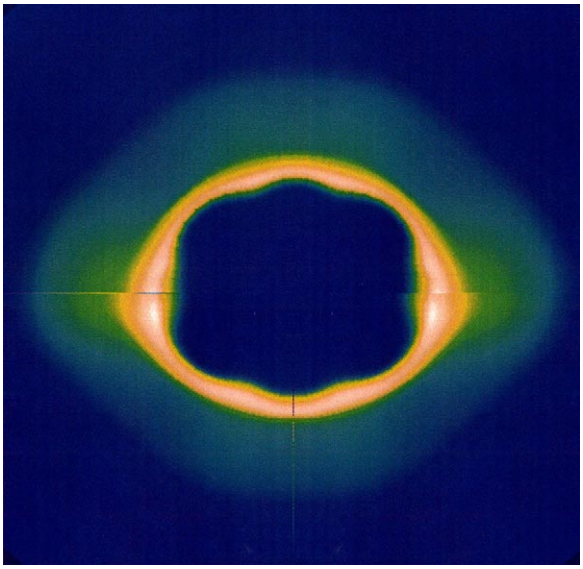

Fig 3 Imploded core at ignition time from integrated 2D HYDRA hohlraum simulations both with (top) and without (bottom) fill-tube plasma included. The implosion is slightly more sausage when the fill-tube plasma is included.

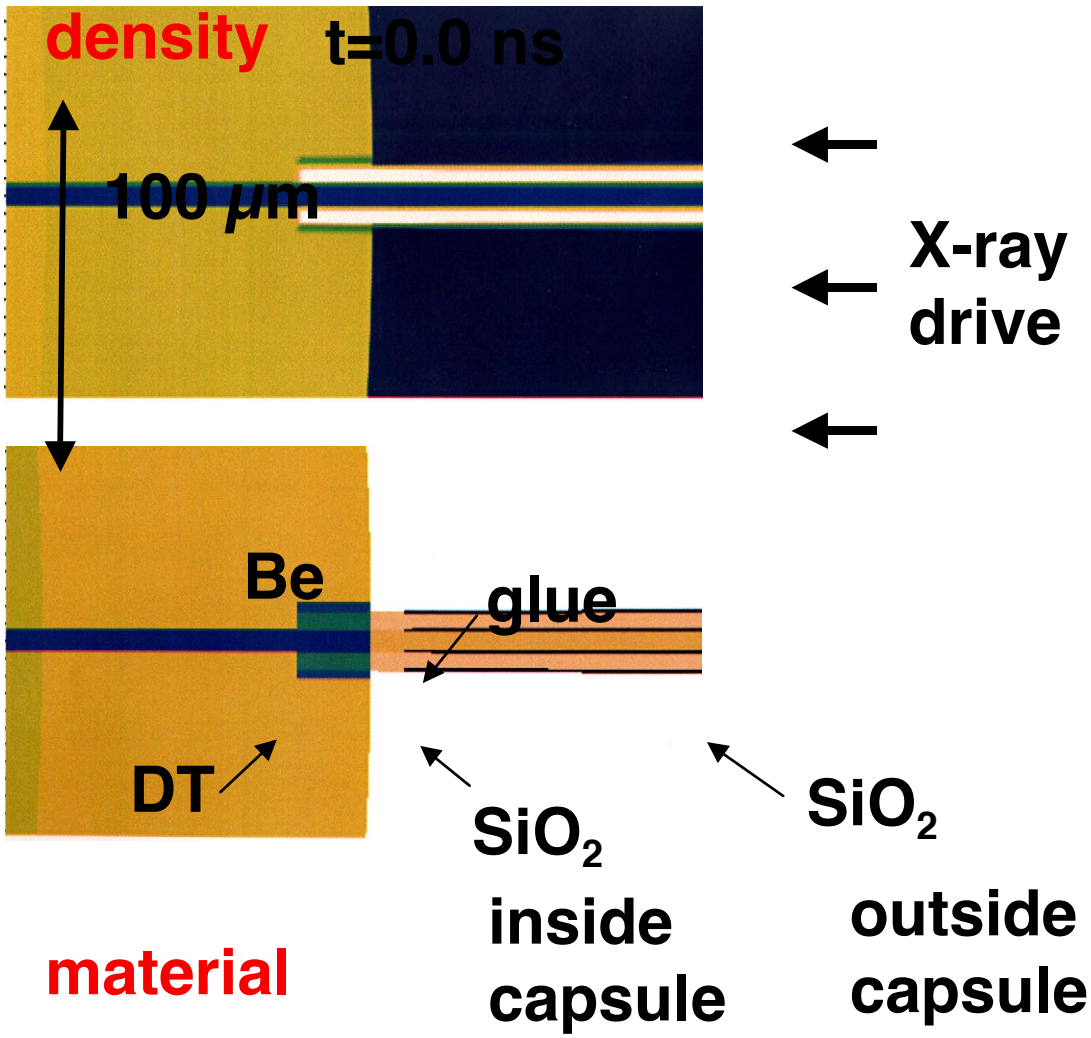

Fig 4a) density plot (top) and material plot (bottom) of the capsule in the region of the fill tube at t=0

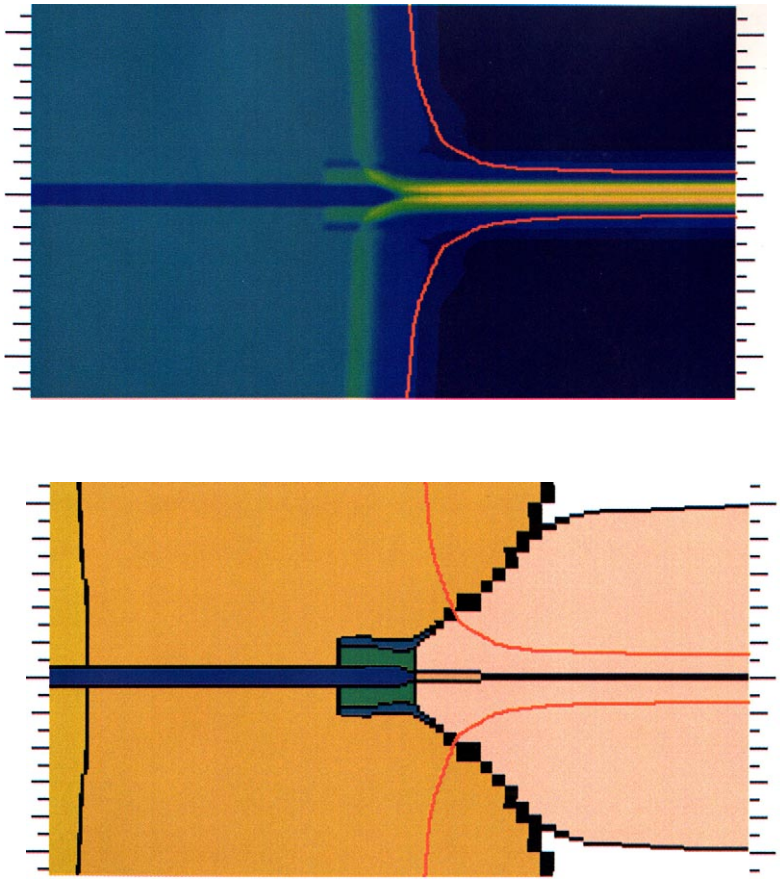

Fig 4b) As 4a) but at t =1 ns. The red line shows the 10% TR4 contour and is a good indicator of how far the radiation is penetrating. Note that the glass outside the ablator is strongly shielding the capsule directly below it, and that this extends some way away from the tube surface.

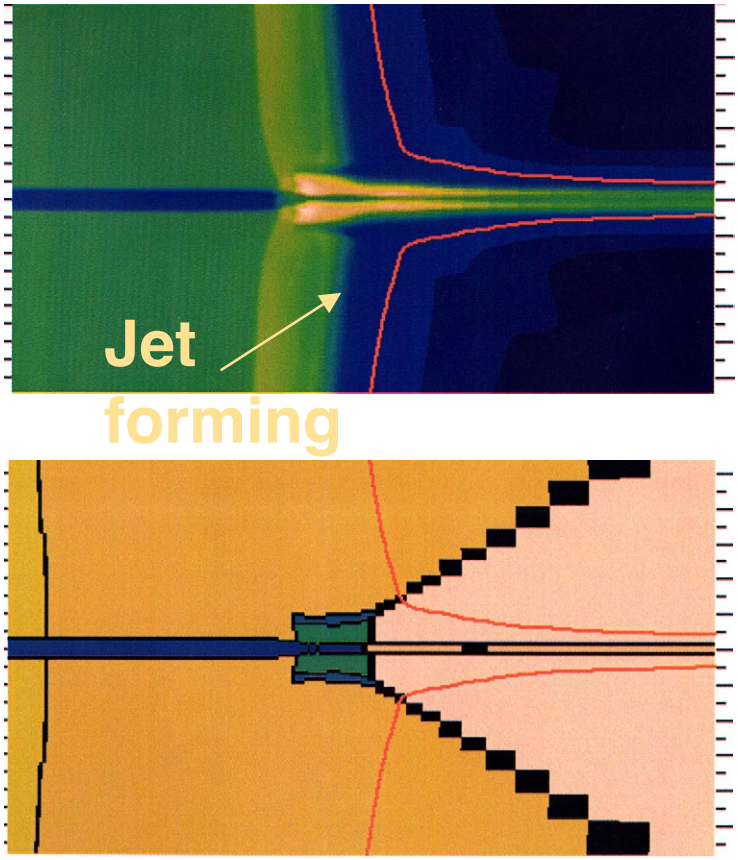

Fig 4c) As 4a) but at 2.5 ns. Note the shielding is continuing, and the shock in the Be has overrun the glass tube, and is crushing the fill hole. This is about to forma jet.

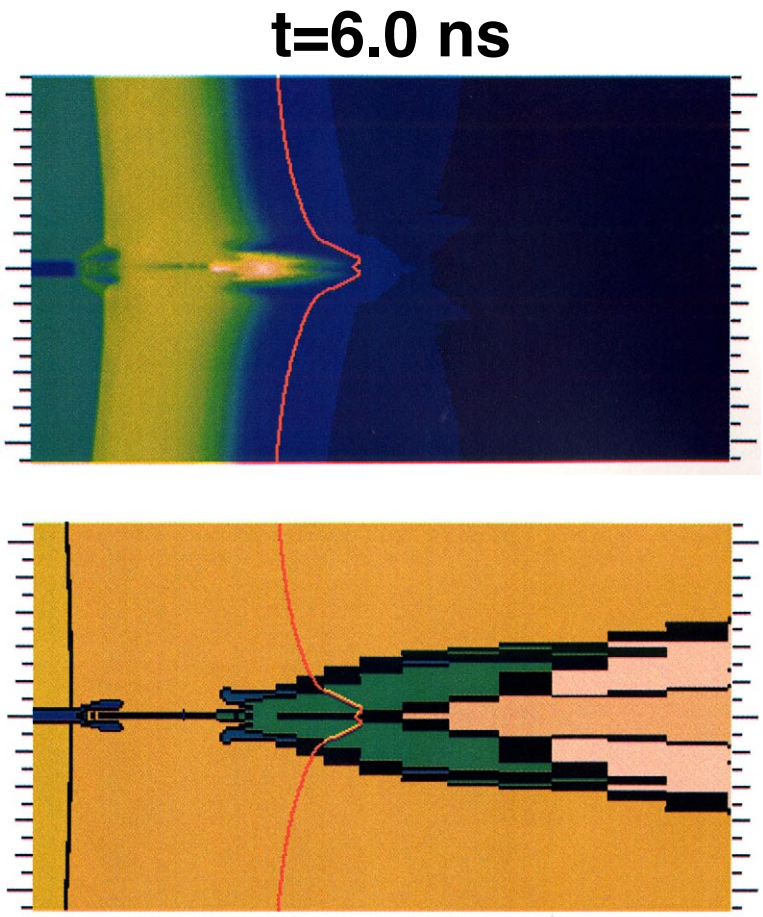

Fig 4 d). As 4a) but at 6ns. The tube in the hohlraum has burned through and the glass originally inside the ablator is being ablated. The jet in the fill hole is now clearly observable.

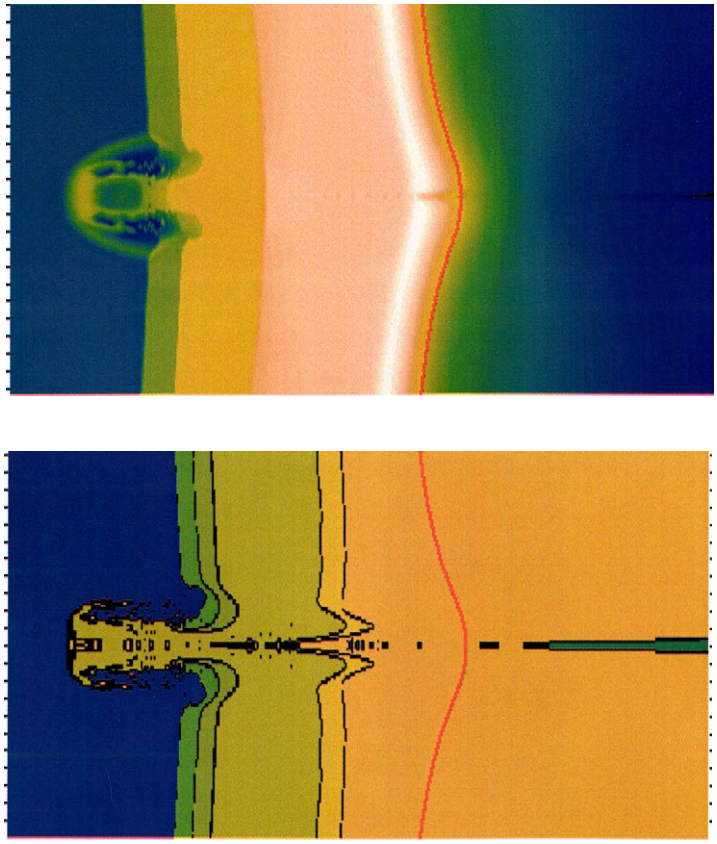

Fig 4e). As 4a but at 12 ns. The jet is propagating into the DT ice and all the fill-tube assembly has been ablated. There are now no further sources of perturbation.

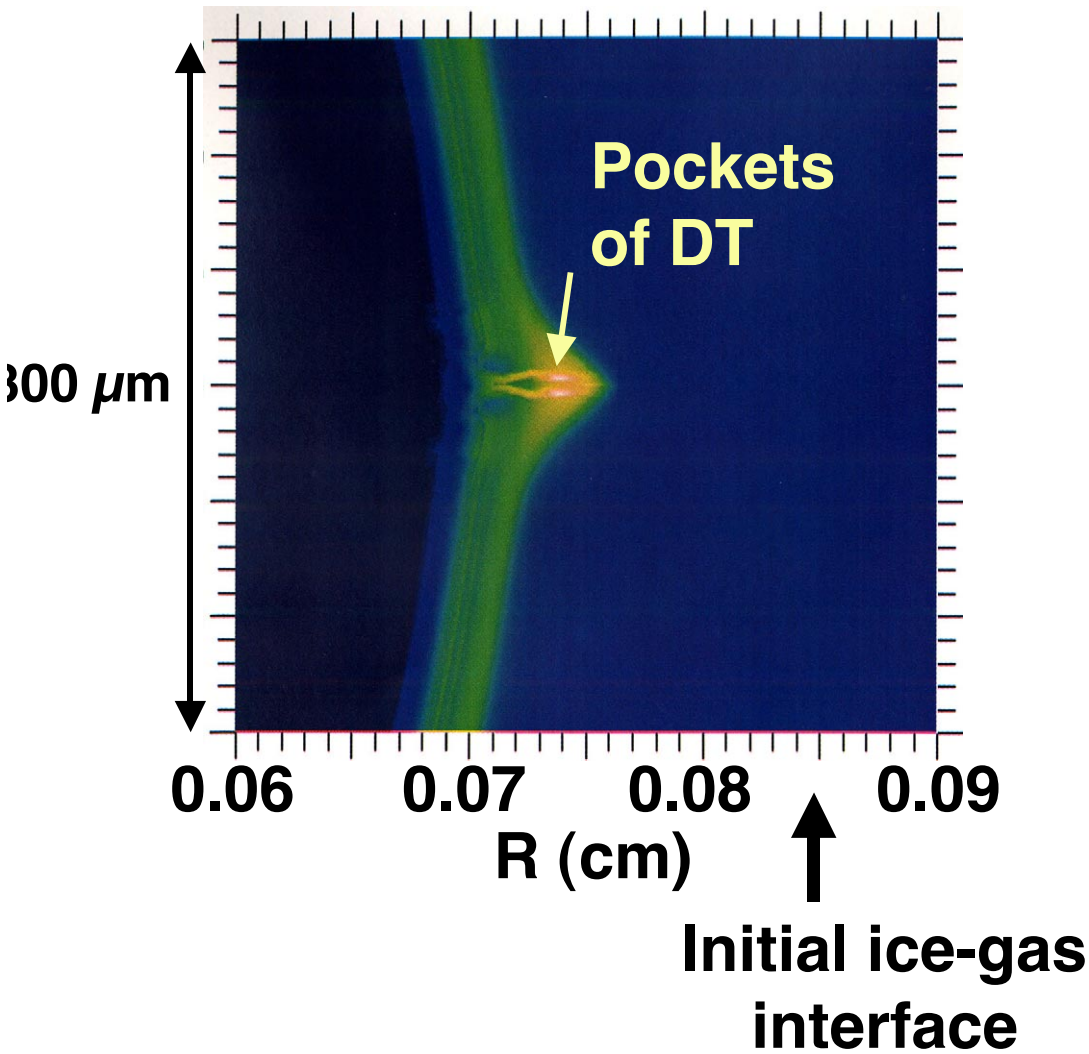

Fig 4f) Density map near the peak of the drive at 15 ns the shell is beginning to accelerate inwards. The jet has been swept up and despite the complex flow in the early phases of the implosion, the perturbation settles into a preferred mode which is much larger than the initial size of the tube. This simply continues to grow until stagnation.

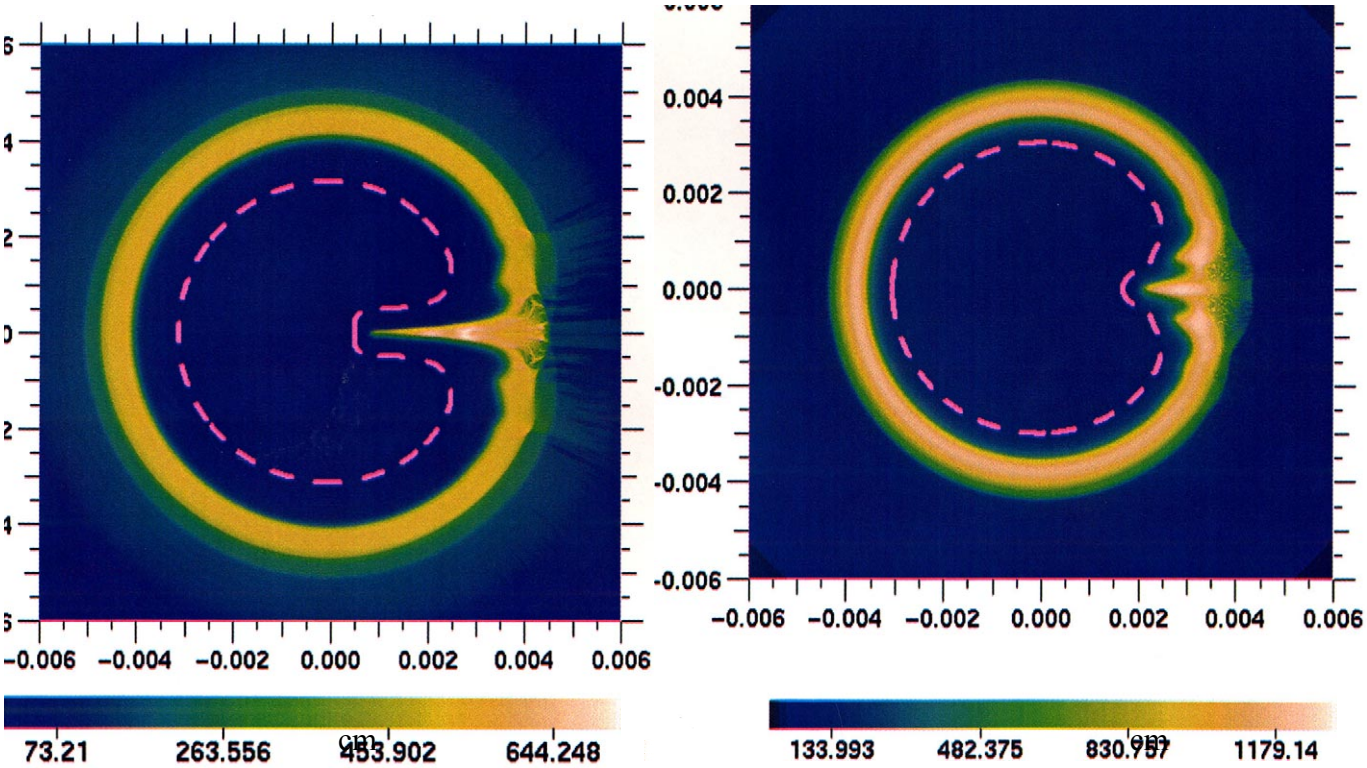

g/cc g/cc

Fig 4g) Density maps of the imploded core at time of maximum spike penetration into the hot spot (left) and ignition (right). The dashed line is the 50% peak Ti contour. In the run up to ignition the spike is heavily eroded by thermal conduction from the hot spot.

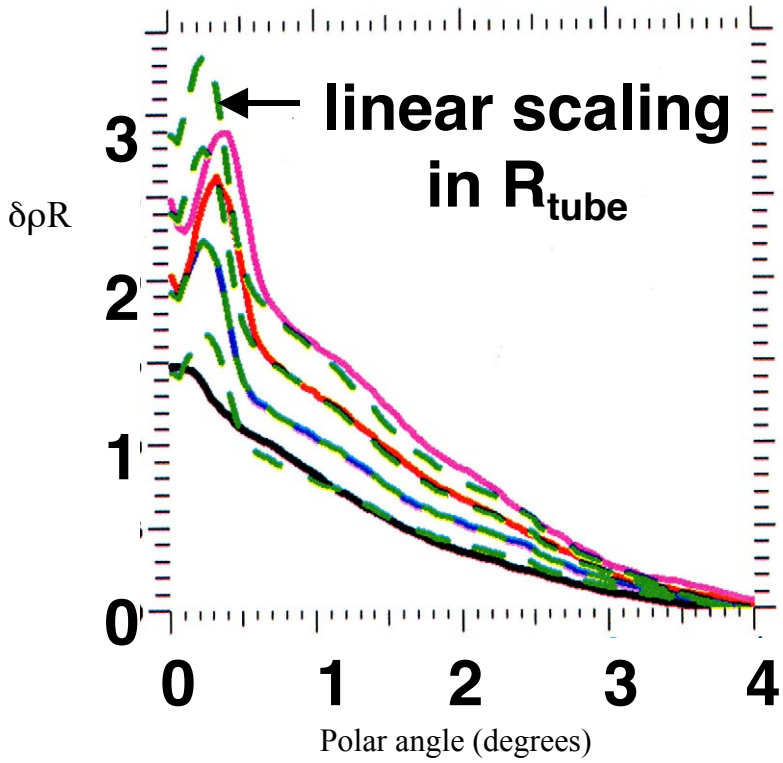

Fig 5a) Fractional ρR perturbation vs polar angle at 15 ns for targets with fill-tubes with initial diameters of 10, 13.5, 17, and 20.2 μm (increasing). Dashed lines are obtained from linearly scaling the second lowest curve (13.5 μm tube) with the tube diameter and demonstrate linear scaling of the perturbation amplitude with tube diameter.

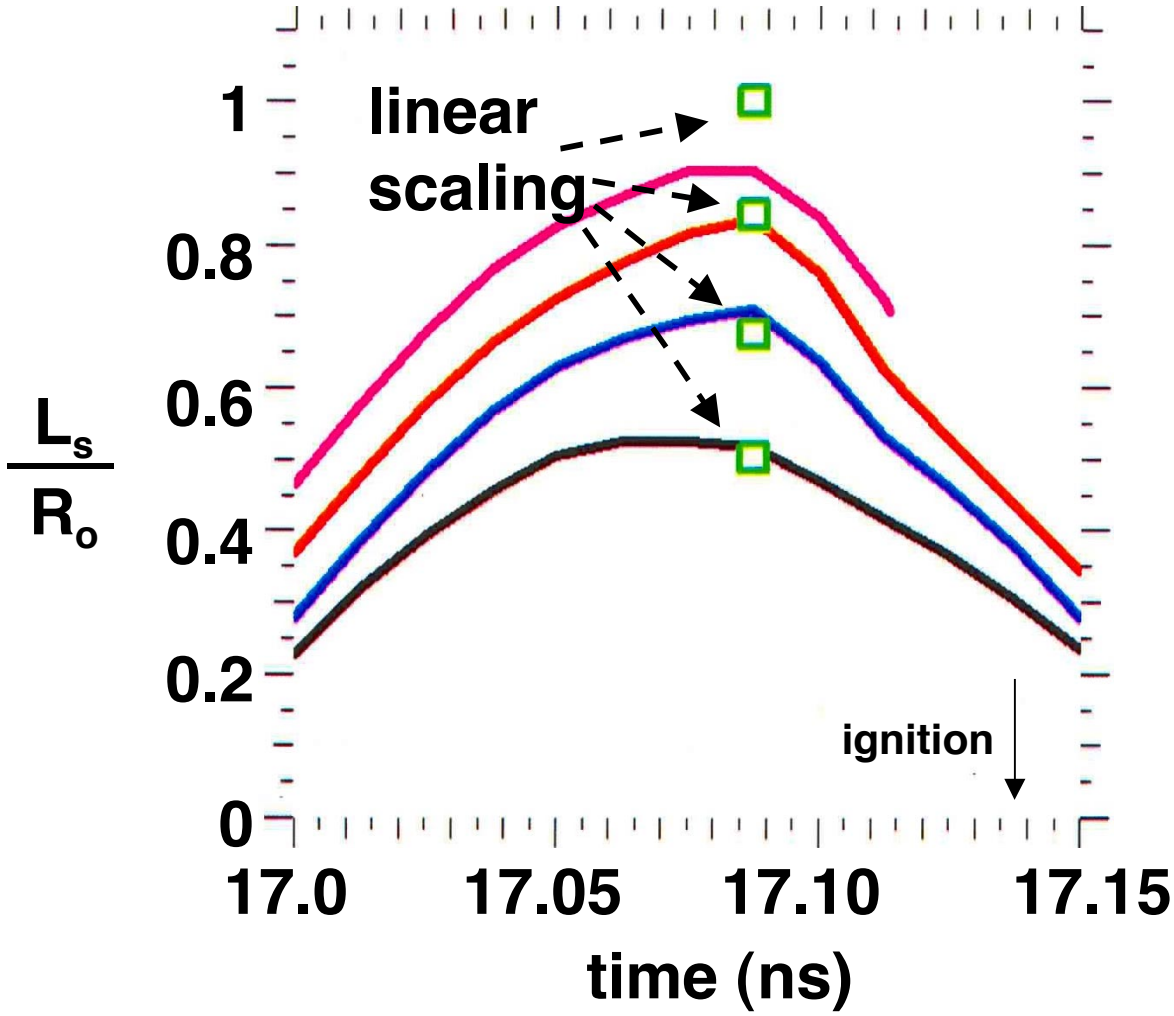

Fig 5b) Spike size in units of the unperturbed hot spot radius defined at the 50% peak Ti contour near ignition for targets with fill-tubes with initial diameters of 10, 13.5, 17, and 20.2 μm (increasing). The squares show linear scaling which is close to what is observed.

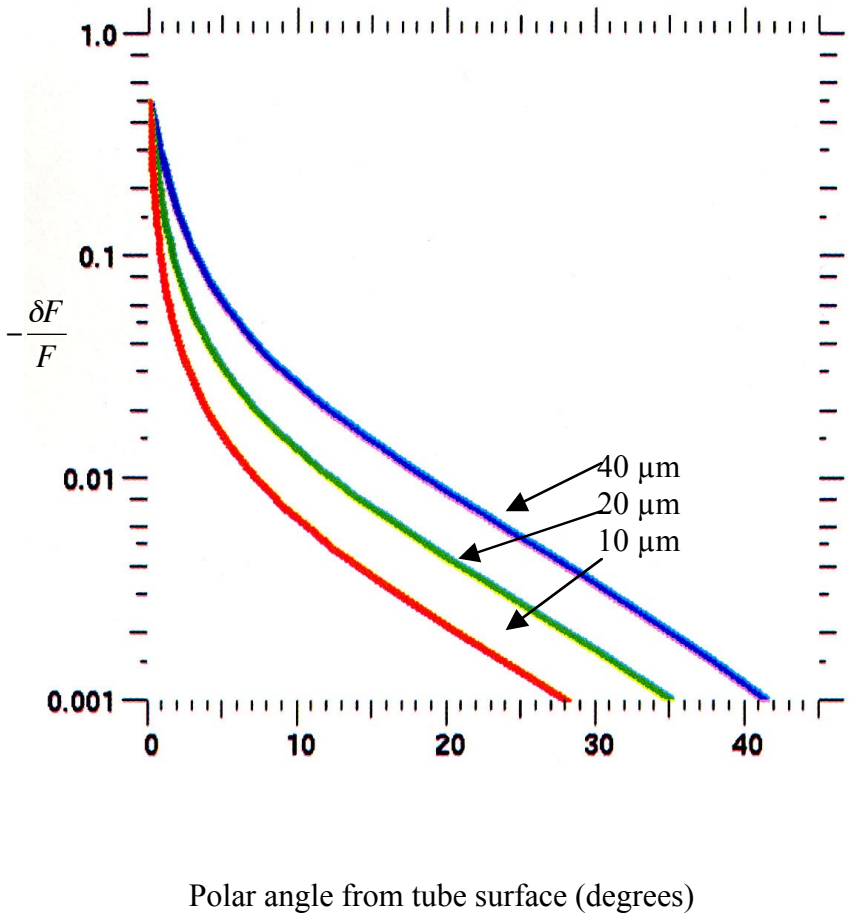

Fig 6. Flux deficit vs polar angle for opaque fill-tubes of 10, 20, and 40 µm diameter. Shadowing is surprisingly large at large distances from the tube.

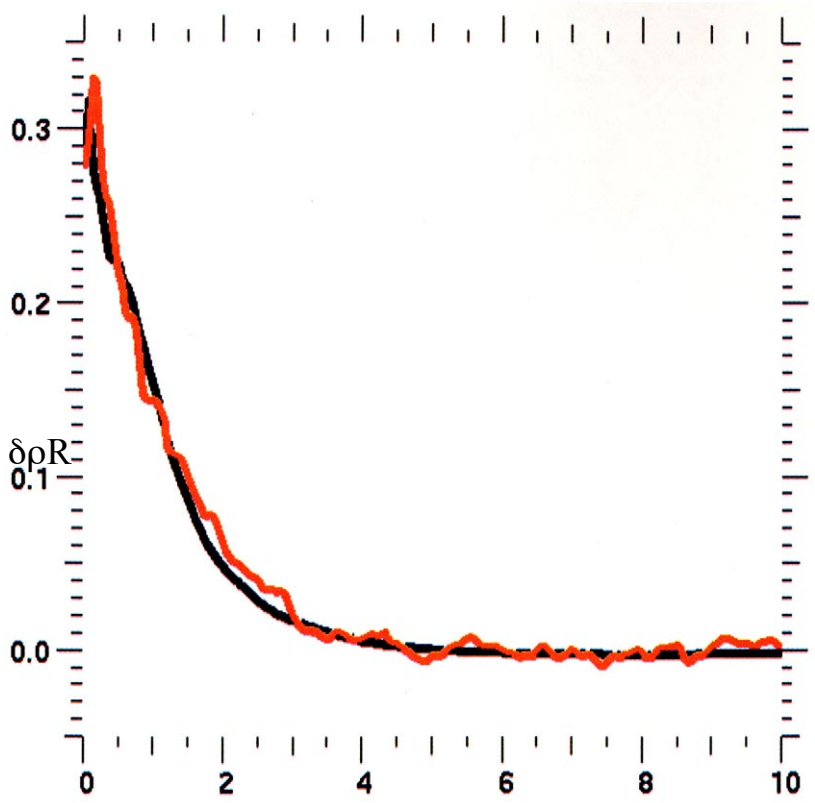

Polar angle (degrees)

Fig 7. Comparison of drR vs polar angle at 13 ns after all sources of perturbation have occurred for Hydra IMC and diffusion calculations for nearly identical initial conditions. The noisier curve is the IMC result and is almost indistinguishable from the diffusion calculation.

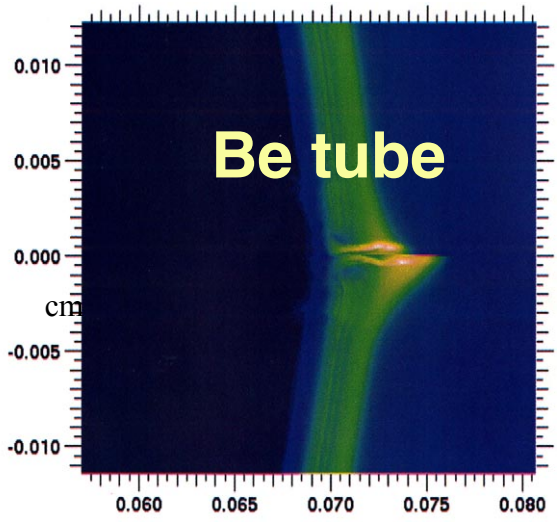

Radius (cm)

Fig 8. Density plot at 15 ns comparing the results from a Be fill tube (top) and glass fill tube (bottom, case B). These were otherwise identical except for the glue layer that was omitted from the Be case but this is not important. The perturbation seed is clearly much reduced in the Be tube case.